

Experiments with Geiger-Müller Counter

Maitrey Sharma*

School of Physical Sciences, National Institute of Science Education and Research, HBNI, Jatni-752050, India

(Dated: March 15, 2022)

In this experiment, we perform various experiments using the Geiger-Müller Counter and understand the working of the electronics and physics behind it. We first examine the characteristic curve of the G-M tube and study the terminology involved there. Then we move on to the gamma radiation and how its intensity depends with distance. Then we indulge ourselves in the statistical analysis of the data obtained through a G-M counter experiment as we study the randomness of radioactive decay. Afterwards, we study the efficiency of our G-M counter and how it varies with gamma or beta source. Then we perform the Feather analysis due to Norman Feather, who contributed to the discovery of neutron with Chadwick. We then move on to study the phenomena of backscattering of the beta particles. After this, we encounter the phenomena of Bremsstrahlung and how it is produced. Finally we measure the short half-life of a given radioactive source.

I. INTRODUCTION

In 1908 Hans Geiger, under the supervision of Ernest Rutherford at the Victoria University of Manchester (now the University of Manchester), developed an experimental technique for detecting alpha particles. This early counter was only capable of detecting alpha particles and was part of a larger experimental apparatus and used a fundamental ionization mechanism used discovered by John Sealy Townsend between 1897 and 1901, known as the Townsend discharge¹. It was not until 1928 when Geiger and his student Walther Müller developed a sealed tube which used basic ionization principles previously used experimentally. Small and rugged, not only could it detect alpha and beta radiation as prior models had done, but also gamma radiation, giving birth to a practical radiation instrument which could be produced relatively cheaply. As the tube output required little electronic processing, a distinct advantage in the thermionic valve era due to minimal valve count and low power consumption, the instrument achieved great popularity as a portable radiation detector.

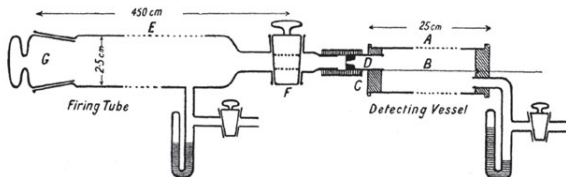


FIG. 1: An early alpha particle counter designed by Rutherford and Geiger.

A Geiger-Müller (G-M) counter is an electronic instrument used for detecting and measuring ionizing radiation. It detects ionizing radiation such as alpha particles, beta particles, and gamma rays using the ionization effect produced in a Geiger-Müller (G-M) tube, which gives its name to the instrument.

The G-M tube is named after Hans Geiger, who invented the principle in 1908 at the University of Manchester, and Walther Müller, who collaborated with Geiger in developing the technique further in 1928 to produce a practical tube that could detect a number of different radiation types. It is a gaseous ionization detector and uses the Townsend avalanche phenomenon to produce an easily detectable electronic pulse from as little as a single ionizing event due to a radiation particle. It is used for the detection of gamma radiation, X-rays, and alpha and beta particles. It can also be adapted to detect neutrons.

A G-M Tube consists of basically an electrode at a positive potential (anode) surrounded by a metal cylinder at a negative potential (cathode). The cathode forms part of the envelope or is enclosed in a glass envelope. Ionizing events are initiated by quanta or particles, entering the tube either through the window or through the cathode and colliding with the gas molecules. The gas filling consists of a mixture of one or more rare gases and a quenching agent. Quenching is the termination of the ionization current pulse in G-M tube. Effective quenching in G-M Tube is determined by the combination of the quenching gas properties and the value of the anode resistor.

II. DESCRIPTION OF THE SET-UP

In this experiment, we will be using the cylindrical “end window” type pf G-M tube construction (figure (2)), which is the usual form of tube for alpha particles, low energy beta particles, and low energy X-rays. This type has a window at one end covered in a thin material through which low-penetrating radiation can easily pass. Mica is a commonly used material due to its low mass per unit area. The other end houses the electrical connec-

* maitrey.sharma@niser.ac.in

¹ The Townsend discharge or Townsend avalanche is a gas ionisation process where free electrons are accelerated by an electric field, collide with gas molecules, and consequently free additional electrons. Those electrons are in turn accelerated and free additional electrons. The result is an avalanche multiplication that permits electrical conduction through the gas.

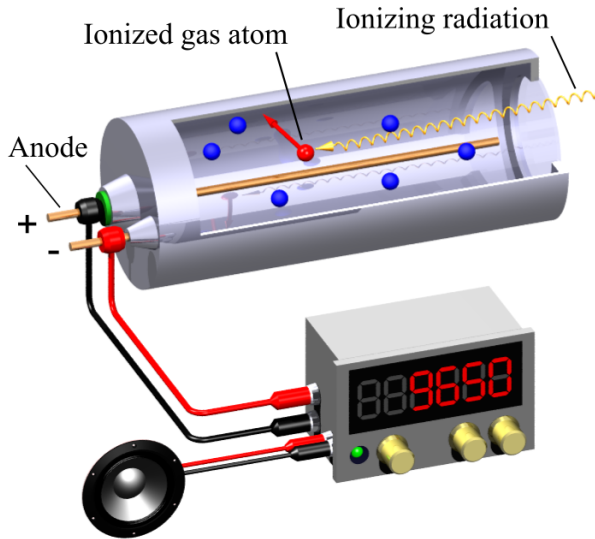


FIG. 2: Diagram of a Geiger counter using an end window tube for low penetration radiation. A loudspeaker is also used for indication



FIG. 3: G-M counting system with End window detector stand and sliding bench

tion to the anode. The complete experimental apparatus is presented in figure (3). The experimental set-up of the counting experiments has several components, each of which are described in this section.

1. **Geiger counting system:** The main counting system device designed around a 8-bit microcontroller chip.
2. **Detector:** GM 120 is a Halogen Quenched End Window G-M Detector used in the experiment. Its operating voltage is approximately 500 V. It has got a very wide plateau length and plateau slope is better than 6% per 100 V. This detector is supplied in a cylindrical PVC enclosure with MHV (miniature high voltage) socket arrangement for applying HV (high voltage) bias voltage.
3. **Stand for the detector:** Stand for G-M tube type SG 200 has been designed to hold PVC enclosed End Window G-M tube. This stand can be housed inside the lead shielding if required. It has both sample and absorber trays. The position of these trays can be adjusted from the end window

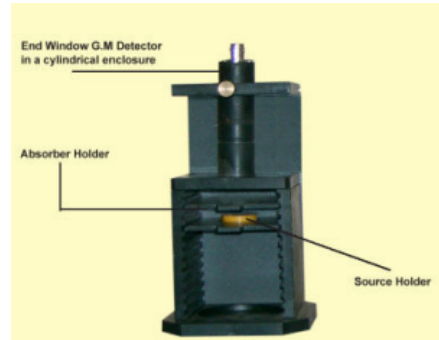


FIG. 4: G-M detector stand

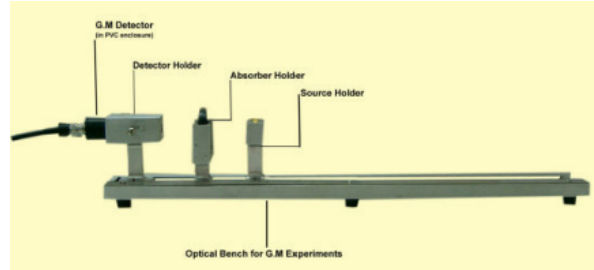


FIG. 5: Sliding bench for the G-M experiments

of the detector. The stand made up of acrylic sheet is precisely milled for sliding-in of sample and absorber trays. Sample tray is designed to hold planchets or disc type radioactive standard source (Beta or Gamma). Aluminium absorber discs can be interposed between the source and the detector for attenuating the radiation as seen by the detector.

Captive screw holds the detector PVC tube to any height. To increase the distance between end window and source one can lift the PVC tube further up which can be held by captive screw. The detector apparatus is presented in figure (4).

4. **Sliding Bench:** This essentially consists of a bench with sliding grooves with a graduated stainless steel scale fixed on one side of it. Scale has gradations both in cm and inches upto 50cm/20 inches. There are three vertical sliding mounts, each for mounting of End Window G-M detector horizontally facing the absorber and source mounts. Each of these mounts can be positioned along the slide scale to have required distance between the end window to the source with absorber mount interposed in between. End Window detector is housed in PVC enclosure with MHV socket fixed on to it. The sliding bench apparatus is presented in figure (5).
5. **Source kits:** These kits contain the radioactive (Beta and Gamma) sources. These are low active disc sources of the order of 0.2 to 3 micro curie for

Beta and Gamma. Gamma source disc is evaporated and sealed inside 25mm (diameter) \times 5mm thick plastic disc. Whereas Beta source disc is evaporated and sealed in a 25mm \times 10mm thick plastic disc and covered with 10mg/ sq.cm aluminised mylar foil.

6. **Aluminium absorber set:** It consists of absorber discs in different thicknesses ranging from 20 to 300 mg/cm.sq. Each of these absorbers is mounted in an individual plastic frame, which exactly fits into the absorber tray holder of the detector stand/sliding bench.
7. **Lead castle:** The Lead Castle is designed to shield the G-M Counters from counting background radiation. This shield is of 40 mm thickness and is built up of six interlocking rings. The top and bottom are covered by similar interlocking discs. A door is fitted in the bottom ring with 150 degree opening to facilitate easy access to the sample holding tray of G-M Stand. The door is fitted with heavy duty hinges and the inside of the lead shield is lined with thin aluminium sheet to minimize scattering.
8. **Absorber/scatterer sets:** The absorber/scatterer set used in the Beta-particle scattering experiment consists of 15 Aluminium foils, the thickness of each foil being 0.05 mm. The one used in the Bremsstrahlung experiment consists of combinations of Aluminium (0.7 mm thick), along with Copper (0.3 mm thick) and Perspex (1.8 mm thick).

III. THE EXPERIMENTS

Before beginning the experiments, it is essential to calculate the present activity rates of the radioactive sources. We know, the activity is given by

$$A = A_0 e^{-\lambda t} = A_0 e^{-(0.693/T_{1/2})t} \quad (1)$$

where A is the present activity, A_0 is the activity on a previous date $T_{1/2}$ is the half-life of the source, t is the elapsed time and λ is the decay constant.

- **Thallium-204 (Beta source):** We have $A_0 = 11 \text{ kBq}$ (in May 2016), $T_{1/2} = 4 \text{ years}$, $t = 5.67 \text{ years}$ (by February 2022), putting these values in equation (1), we get $A = 4120.34 \text{ Bq}$.
- **Strontium-90 (Beta source):** We have $A_0 = 3.7 \text{ kBq}$ (in May 2019), $T_{1/2} = 28.5 \text{ years}$, $t = 2.67 \text{ years}$ (by February 2022), putting these values in equation (1), we get $A = 3467.65 \text{ Bq}$.
- **Caesium-137 (Gamma source):** We have $A_0 = 86 \text{ kBq}$ (in May 2016), $T_{1/2} = 30 \text{ years}$, $t = 5.67 \text{ years}$ (by February 2022), putting these values in equation (1), we get $A = 75446.18 \text{ Bq}$.

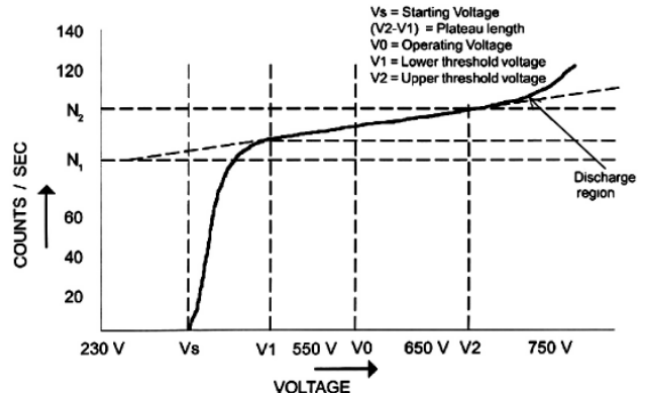


FIG. 6: Typical G-M characteristics

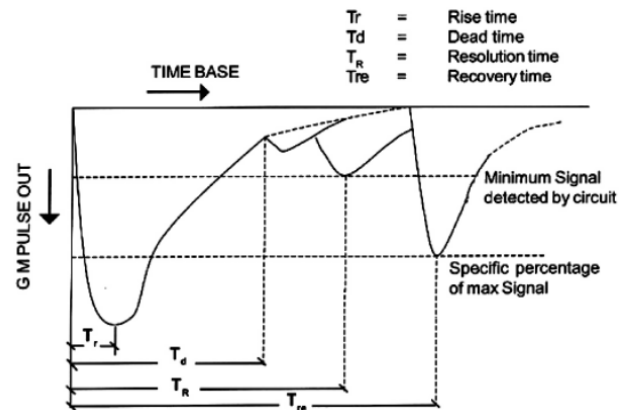


FIG. 7: Typical G-M pulse output as seen on an oscilloscope

A. Characteristics of Geiger-Müller Tube

The first experiment is concerned with the characteristics of the G-M counter. We will study the variations of count-rate with applied voltage and thereby determine the plateau, the operating voltage and the slope of the plateau. The equipment used are the G-M counting system, the end window detector stand, the G-M detector itself and a radioactive source.

There are various operating characteristics of the G-M tube which define how it behaves when irradiated constantly. The lowest voltage applied to a G-M tube at which pulses just appear across the anode resistor (figure (6)) and unit starts counting is called the **starting voltage**, V_s . The section of the G-M characteristic curve constructed with counting rate versus applied voltage (with constant irradiation) over which the counting rate is substantially independent of the applied voltage is called the **plateau** and the voltage range over which it extends is called the **plateau length**. The slope of the plateau line is referred as the **plateau slope**. The two voltages, corresponding to the start and the end of the plateau are called the **lower** (V_1) and **upper threshold voltages** (V_2) respectively. The average of these two is taken as

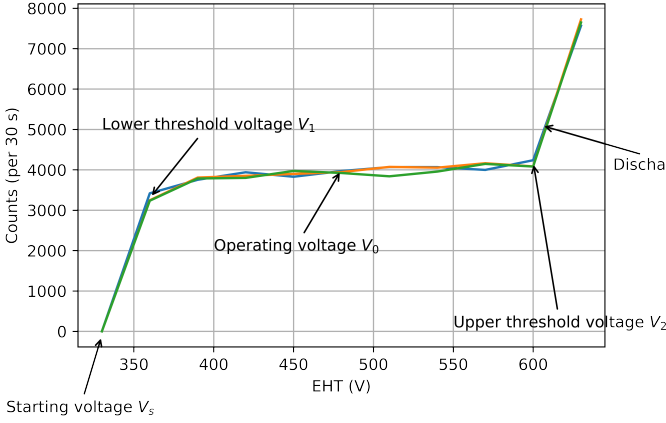


FIG. 8: Experimentally obtained G-M characteristics curve for Cs-137

the ***operating voltage***, V_0 of the G-M tube.

The radioactive source used is the Cs-137 gamma source. The observations made are tabulated in table (I). The background counts represent the counts in absence of the source, due to cosmic rays or any other sources in the location of experiment.

1. Calculations

From the tabulated readings (I), we have lower threshold voltage (the starting voltage of the plateau, just after the rising edge of knee), $V_1 = 360\text{ V}$. Similarly, the upper threshold voltage (just before the start of the discharge region), $V_2 = 600\text{ V}$. The plateau length is $VPL = V_2 - V_1 = 240\text{ V}$. The operating voltage is $V_0 = 480\text{ V}$. Corresponding to the three sets of data, we have three plateau slopes. The general expression of slope (expressed as the percent change in count rate per 100 volts change in applied voltage in the plateau region) is given by

$$m = \frac{2(N_2 - N_1) \times 10^4}{(N_2 + N_1)(V_2 - V_1)} \% \quad (2)$$

where N_1 and N_2 are the count rates at the lower and the upper limits of the plateau.

The three slopes (expressed as the percent change in count rate per 100 volts change in applied voltage in the plateau region) so obtained are $m_1 = 8.92\%$, $m_2 = 9.53\%$ and $m_3 = 9.64\%$.

2. Error Analysis

We calculate the error found in slope as the standard deviation of m_i 's. The formula of standard deviation for

a sample of data is

$$\sigma = \sqrt{\frac{\sum(x_i - \mu)^2}{N - 1}} \quad (3)$$

where x_i 's are the observations, μ is the mean and N is the number of observations. From here we get $\sigma = 0.39\%$. The mean slope comes out to be $m = 9.36\%$.

3. Discussions

1. From the plateau, it can be noticed that mid point of the characteristics of the G-M tube is defined as operating voltage and is to be used for counting applications. The tube is operated at this voltage when used in Radiation Monitors for measurements.
2. This experiment can be repeated with Beta source by keeping the source slightly away from the end window when compared to gamma source. From this, one could notice that with Beta source, the efficiency of the detector increases.
3. Also one can notice that with higher count rates, plateau slope increases.

4. Results

1. The final slope (expressed as the percent change in count rate per 100 volts change in applied voltage in the plateau region) obtained was $9.36 \pm 0.39\%$.
2. The slope obtained so is under 10% which is desirable and well within the margin of error.

B. Inverse Square Law for Gamma rays

According to the inverse square law, intensity of gamma radiation falls inversely as square of the distance. The equipment required for this experiment are the G-M counting system, the end window detector stand, the G-M detector itself and a gamma source (Cs-137). The set-up arrangement is given in figure (9).

Before beginning the experiment, we take (5) readings for the background counts and compute the average background counts in 60 seconds as $(49+61+57+68+65)/5 = 60$. The operating voltage, as determined in first experiment (III A), is $V_0 = 480\text{ V}$.

1. Data Analysis

If the count rate obeys the inverse square law, it can be easily be shown that the product $C = Rd^2$ is a constant. The results of the product (Rd^2) are shown in the

TABLE I: Readings for the G-M characteristics experiment

EHT (V)	Background counts (30 s)			Counts (30 s)			Corrected Counts (30 s)		
	0	0	0	0	0	0	0	0	0
330	0	0	0	0	0	0	0	0	0
360	14	36	35	3432	3282	3270	3418	3246	3235
390	27	26	32	3780	3834	3817	3753	3808	3785
420	32	25	23	3971	3876	3823	3939	3851	3800
450	33	33	43	3861	3931	4015	3828	3898	3972
480	44	28	33	4013	3972	3954	3969	3944	3921
510	23	27	27	4091	4099	3866	4068	4072	3839
540	31	25	40	4098	4078	3996	4067	4053	3956
570	40	30	22	4037	4193	4168	3997	4163	4146
600	30	29	23	4267	4113	4104	4237	4084	4081
630	66	56	46	7633	7781	7694	7567	7725	7648

TABLE II: Readings for the inverse square law experiment

Distance, d (cm)	Counts (60 s)	Corrected counts (60 s)	Net count rate, R (s^{-1})	Product ($C = Rd^2$)	Transformation ($1/d^2$ in $1/m^2$)
2	4409	4349	72.48	290	2500
2.5	3698	3638	60.63	379	1600
3	2955	2895	48.25	434	1111
3.5	2527	2467	41.12	504	816
4	2162	2102	35.03	561	625
4.5	1743	1683	28.05	568	494
5	1514	1454	24.23	606	400
5.5	1332	1272	21.20	641	331
6	1102	1042	17.37	625	278
6.5	1019	959	15.98	675	237
7	888	828	13.80	676	204

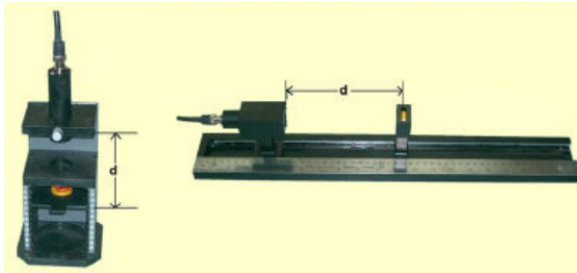
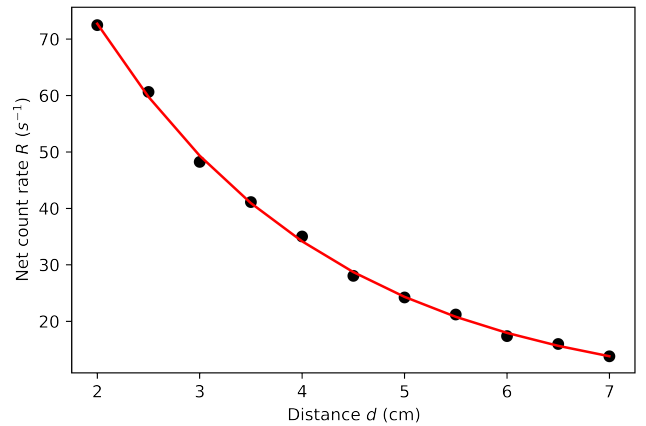


FIG. 9: Detector, G-M stand/holder and source arrangement

table above; allowing for statistical fluctuations, the results obey this law, with a mean value of $C = 542$. Then the observed net count rate as a function of distance is given by

$$R_d = \frac{542}{d^2} \quad (4)$$

An alternative analysis method involves transforming

FIG. 10: Plot of net count rate R against distance d

the data so that the results lie on a straight line. For this purpose *Net Count Rate (R) Vs. Reciprocal of the distance square ($1/d^2$)* are plotted (figure (11)). This

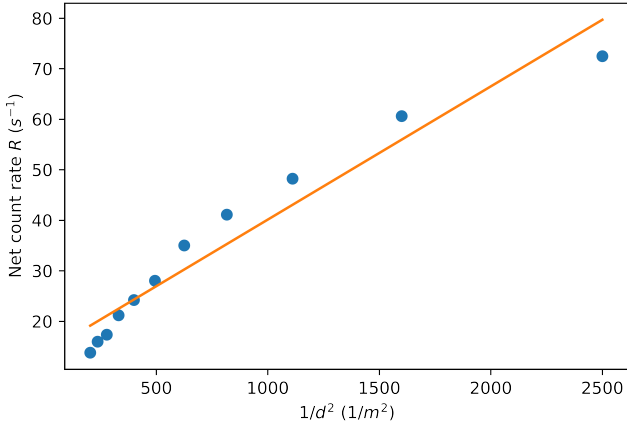


FIG. 11: Plot of net count rate R against inverse of distance square $1/d^2$

TABLE III: The $\log d$ and $\log R$ values for inverse square law experiment

Distance, d (cm)	$\log d$	Net count rate, R (s^{-1})	$\log R$
2	0.301	72.48	1.860
2.5	0.398	60.63	1.783
3	0.477	48.25	1.683
3.5	0.544	41.12	1.614
4	0.602	35.03	1.544
4.5	0.653	28.05	1.448
5	0.699	24.23	1.384
5.5	0.740	21.20	1.326
6	0.778	17.37	1.240
6.5	0.813	15.98	1.204
7	0.845	13.80	1.140

will be a straight line passing through the origin $(0, 0)$ as this point corresponds to a source-detector distance of infinity. Gradient can be estimated easily from the *Net Count Rate* (R) corresponding to a value of $(1/d^2)$.

Another way of data analysis is by plotting these values on a log-log graph sheet or compute log values and plot them on a linear graph sheet (12).

2. Discussions

- Gamma radiation is part of the electromagnetic spectrum. It is not absorbed by the air, but its intensity decreases because it spreads out. Therefore, the intensity varies with the inverse square of distance: it follows an inverse square law.
- This is the same law that governs all electromagnetic radiation (like the Sun's luminosity). This is some evidence that gamma radiation is part of the electromagnetic spectrum.
- In order to protect yourself from gamma radiation

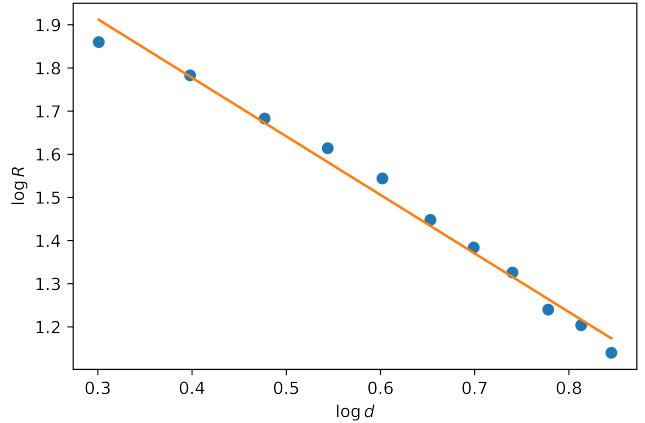


FIG. 12: Plot of $\log R$ against $\log d$

the best thing to do is to move farther away. At 10 times the distance you will be 100 times as safe.

3. Results

- The plot between net count rate and distance was expectedly obtained as an exponentially decreasing curve.
- The plot between net count rate and inverse square of distance was expectedly obtained as a straight line curve (with a positive slope).
- The log-log plot between net count rate and distance was expectedly obtained as a straight line curve (with a negative slope).

C. Nuclear Counting Statistics

Radioactive decay is a random process. Consequently, any measurement based on observing the radiation emitted in a nuclear decay is subject to some degree of statistical fluctuations. These inherent fluctuations are unavoidable in all nuclear measurements. The term counting statistics includes the framework of statistical analysis required to process the results of nuclear counting experiments and to make predictions about the expected precision of quantities derived from these measurements.

Although each measurement (number of decays in a given interval) for a radioactive sample is independent of all previous measurements (due to randomness of the process), for a large number of individual measurements the deviation of the individual count rates from the average count rate behaves in a predictable manner. Small deviations from the average are much more likely than large deviations. These statistical fluctuations in the nuclear decay can be understood from the statistical models utilizing Poisson distribution or Gaussian (Normal) distribution. If we observe a given radioactive nucleus for a

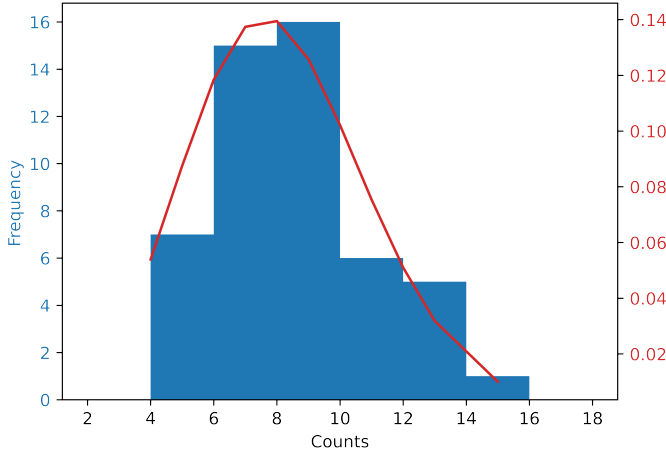


FIG. 13: Histogram for background counts and overlaid Poisson curve

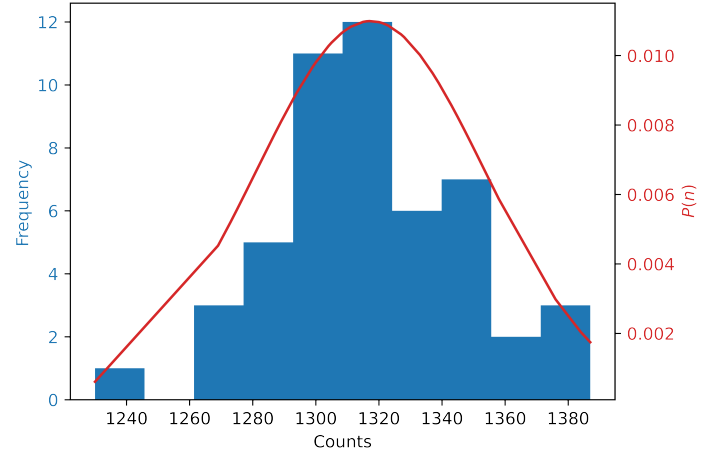


FIG. 14: Histogram for counts with source and overlaid Gaussian curve

time t and define the success as “the nucleus decays during the process” then the probability of success p is given by $(1 - e^{-\lambda t})$. The Poisson distribution applies when the success probability p is small and the number successes (i.e. number of counts measured) is also small (say < 30). In practical terms, this condition implies that we have chosen an observation time that is small compared with the half-life of the source. When the average number of the number of successes becomes relatively large (say > 30) we can utilize the Gaussian model of distribution. Since in most of the cases the count rates are reasonably large (few tens of counts per second) the Gaussian model has become widely applicable to many problems in counting statistics. On the other hand the Poisson distribution is applicable in the case of background counts.

The Poisson distribution function is given by

$$P(N) = \frac{\bar{N}^N e^{-\bar{N}}}{N!} \quad (5)$$

where \bar{N} is the experimental mean. The corresponding standard deviation is given by $\sigma_p = \sqrt{\bar{N}}$.

The Gaussian distribution function is given by

$$P(N) = \frac{1}{\sqrt{2\pi\bar{N}}} \exp\left(-\frac{(N - \bar{N})^2}{2\bar{N}}\right) \quad (6)$$

Here the standard deviation is given by $\sigma_G = \sqrt{\bar{N}}$.

The equipment required for this experiment are the G-M counting system, the end window detector stand, the G-M detector itself and a radioactive source.

1. Discussions

1. The results follow a Poisson distribution on which practically all radioactivity measurements are based. The results show that the mean value N

is equal to the variance σ^2 ; this is characteristic of the Poisson distribution. The variance in any measured number of counts is therefore equal to the mean value of counts.

2. The square root of variance, the standard deviation is a measure of the scatter of individual counts around the mean value. As a thumb rule we can say that approximately 2/3 of the results are within one standard deviation of the mean value i.e., within the interval $[(N - \sigma) \text{ and } (N + \sigma)]$, where $\sigma\sqrt{N}$. Conversely, given the result from an individual measurement, the unknown *true* count lies within the interval $[N - \sqrt{N} \text{ and } N + \sqrt{N}]$ with a probability of approximately 2/3.
3. The above measured results of mean, variance and standard deviation follow Poisson distribution. Results show that the mean value (N) is almost equal to the variance (σ^2) which is characteristic of the Poisson distribution.
4. The variance in any measured number of counts is therefore equal to the mean value of counts.

2. Results

1. For the background counts, the histogram and Poisson distribution were obtained as expected.
2. For the counts with source, the histograms and the Gaussian distribution were obtained as expected.

D. Efficiency of Geiger-Müller Detector

By knowing the activity of a gamma source, it is possible to record counts with the source for a known preset

TABLE IV: Nuclear Counting Statistics

Background Counts	Poisson Distribution value	Counts with source	Gaussian distribution value
4	0.0539	1230	0.0006
4	0.0539	1269	0.0045
4	0.0539	1273	0.0052
5	0.0875	1275	0.0056
5	0.0875	1278	0.0061
5	0.0875	1281	0.0067
5	0.0875	1281	0.0067
6	0.1184	1287	0.0077
6	0.1184	1289	0.0081
6	0.1184	1293	0.0088
6	0.1184	1293	0.0088
6	0.1184	1294	0.0089
6	0.1184	1299	0.0097
6	0.1184	1300	0.0098
6	0.1184	1300	0.0098
6	0.1184	1304	0.0103
7	0.1374	1305	0.0104
7	0.1374	1305	0.0104
7	0.1374	1308	0.0106
7	0.1374	1308	0.0106
7	0.1374	1309	0.0107
7	0.1374	1309	0.0107
8	0.1395	1311	0.0108
8	0.1395	1315	0.0110
8	0.1395	1316	0.0110
8	0.1395	1317	0.0110
8	0.1395	1320	0.0110
9	0.1258	1320	0.0110
9	0.1258	1320	0.0110
9	0.1258	1321	0.0109
9	0.1258	1322	0.0109
9	0.1258	1323	0.0109
9	0.1258	1327	0.0106
9	0.1258	1327	0.0106
9	0.1258	1328	0.0105
9	0.1258	1333	0.0100
9	0.1258	1337	0.0095
9	0.1258	1339	0.0092
10	0.1022	1343	0.0086
10	0.1022	1345	0.0082
10	0.1022	1347	0.0079
10	0.1022	1349	0.0075
11	0.0754	1349	0.0075
11	0.0754	1351	0.0072
12	0.0510	1355	0.0064
12	0.0510	1358	0.0059
12	0.0510	1358	0.0059
13	0.0319	1376	0.0030
13	0.0319	1384	0.0020
15	0.0100	1387	0.0017

time and estimate the efficiency of the G-M detector. We then calculate the efficiency of the detector for a beta source with the only difference being, here we place Beta source about 2 cm close to the end window and calculate *intrinsic efficiency* (which do not take geometry factor into consideration).

The equipment required for this experiment are the G-

M counting system, the end window detector stand, the G-M detector itself in a cylindrical enclosure, radioactive sources and necessary connecting cables.

TABLE V: Reading for determination of efficiency of the G-M counter

#	Gamma source, Cs-137				Beta source, Tl-204			
	Background (100 s)	Counts (100 s)	Counts (100 s)	Net count rate, R_n (s^{-1})	Background (100 s)	Counts (100 s)	Counts (100 s)	Net count rate, R_n (s^{-1})
1	102	854		7.52	115	4011		38.96
2	109	802		6.93	108	3922		38.14
3	97	877		7.80	110	3930		38.20
4	92	842		7.50	105	3890		37.85
5	110	824		7.14	107	3956		38.49

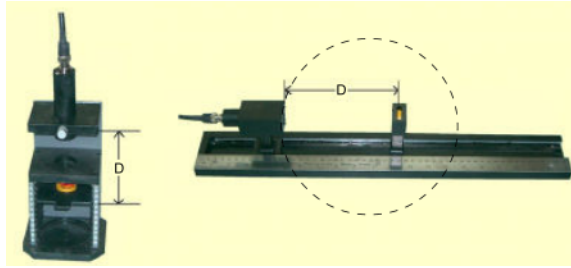


FIG. 15: Detector source arrangement for efficiency calculation for a gamma source

1. Data Analysis

Gamma source emits radiation isotropically in all directions (4Π geometry). However only fraction of it is received by the end window detector. This fraction is given by

$$\frac{\Pi d^2 / 4}{4\Pi D^2} = \frac{d^2}{16D^2} \quad (7)$$

where D is the distance from source holder to end window and d is the diameter of end window.

The present activity (A) of the gamma source used for this experiment is 75.45 kBq. This gamma source is radiating isotropically in all directions. A fraction of this only is entering the G-M Tube, which is given by

$$R = A \times \frac{d^2}{16D^2} \quad (8)$$

For our experiment, $D = 10\text{ cm}$ and $d = 3\text{ cm}$. Thus $R = 424.38\text{ Bq}$. Now average net count rate R can be found by calculating the mean of the values for R given in table (V). For Cs-137, average count rate is given by 7.38 Bq. Now the efficiency is given by

$$E = \frac{CPS}{DPS} = \frac{R_n}{R} \quad (9)$$

where CPS is counts per second and DPS is the dis-integrations per second falling on the detector window. Thus, efficiency of the G-M counter for gamma source, Cs-137 is

$$E = \frac{R_n}{R} = \frac{7.38}{424.38} = 1.74\% \quad (10)$$

Now to calculate the intrinsic efficiency of the beta source, we have average net count rate $R = 38.33\text{ Bq}$. The present activity as calculated earlier is $A = 4120.34\text{ kBq}$. Thus, efficiency is

$$E = \frac{CPS}{DPS} = \frac{38.33}{4120.34} = 0.93\% \quad (11)$$

2. Discussions

1. By knowing the efficiency of the G-M detector for a particular Gamma energy (at a specified distance and geometry), one can further calculate the following parameters, namely activity of the source as on the day of experimentation (of course it is assumed that activity of the standard is known as on the date of manufacture), and also the activity of the unknown source if any with the same energy.
2. It can be noticed that End Window detector will have much better efficiency for Beta Source compared to a gamma source.
3. By knowing efficiency for a Beta source , if an unknown activity Beta source is kept for counting one can calculate and find out its activity.

3. Results

1. The efficiency of the G-M counter for gamma source was found to be 1.74%.
2. The efficiency of the G-M counter for beta source was found to be 0.93%.

E. Feather Analysis

The purpose of Feather analysis is to carry out the absorption studies on β -rays with the aid of a G-M Counter and hence to determine the end point energy of β -rays emitted from a radioactive source.

The equipment required for this experiment are the G-M counting system, the end window detector stand, the G-M detector itself, beta source and Aluminium absorber kit.

TABLE VI: Readings for Feather Analysis experiment for Tl-204

Absorber Thickness (mm)	Absorber Thickness (mg cm^{-2})	Counts (180 s)	Net Counts
0	0	7412	7217
0.06	16.26	5403	5208
0.12	32.52	4132	3937
0.18	48.78	3196	3001
0.24	65.04	1893	1698
0.3	81.3	1897	1702
0.36	97.56	1521	1326

TABLE VII: Readings for Feather Analysis experiment for Sr-90

Absorber Thickness (mm)	Absorber Thickness (mg cm^{-2})	Counts (100 s)	Net counts
0	0	4781	4673
0.06	16.26	4335	4227
0.12	32.52	4120	4012
0.18	48.78	3737	3629
0.24	65.04	3689	3581
0.3	81.3	3610	3502
0.36	97.56	3233	3125
0.42	113.8	3134	3026
0.48	130.1	3323	3215
0.54	146.3	2900	2792
0.66	178.9	2618	2510
0.72	195.1	2405	2297
0.78	211.4	2252	2144
0.9	243.9	2021	1913
1.02	276.4	1781	1673

1. Data Analysis

The range of beta particles is given by

$$R_0 = (0.52E_0 - 0.09)\text{g cm}^{-2} \quad (12)$$

Where E_0 is the end point energy of Beta rays from the radioactive source in MeV.

We have the ratio of thickness required to reduce the counts of Beta rays from one source to half to the thickness required for the other source is given by

$$\frac{t_1^{1/2}}{t_2^{1/2}} = \frac{\text{Range of Beta rays from first source}}{\text{Range of Beta rays from second source}} \quad (13)$$

That is

$$\frac{t_1^{1/2}}{t_2^{1/2}} = \frac{R_1}{R_2} \quad (14)$$

Now, end point energy of Tl-204 is 0.764 MeV. Therefore the range of Tl-204, $R_1 = 0.30728 \text{ g cm}^{-2}$. From the figure (16), thickness of Al absorber required to reduce

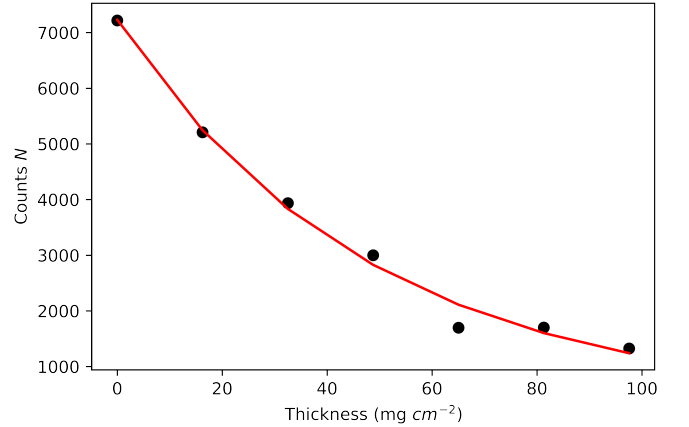


FIG. 16: Feather analysis plot for Tl-204

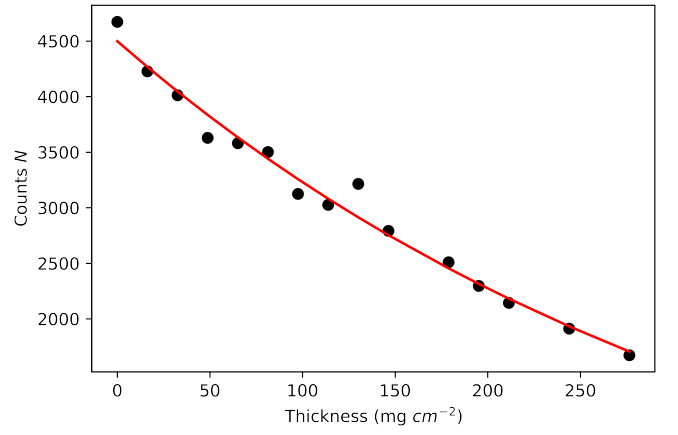


FIG. 17: Feather analysis plot for Sr-90

the count rate of Tl-204 by half, $t_1^{1/2} = 35.7 \text{ mg cm}^{-2}$. From the figure (17), thickness of Al absorber required to reduce the count rate of Sr-90 by half, $t_2^{1/2} = 59.4 \text{ mg cm}^{-2}$. Therefore, we have

$$R_2 = R_1 \times \frac{t_2^{1/2}}{t_1^{1/2}} = 0.511 \text{ g cm}^{-2} \quad (15)$$

Thus, end point energy of Sr-90 is

$$E_2 = \frac{R_2 + 0.09}{0.52} = 1.16 \text{ MeV} \quad (16)$$

2. Results

The end point energy of β -rays from Sr-90 was obtained to be 1.16 MeV.

F. Backscattering of Beta Particles

When Beta Particles collide with matter, absorption may occur. Another possible result is the occurrence of

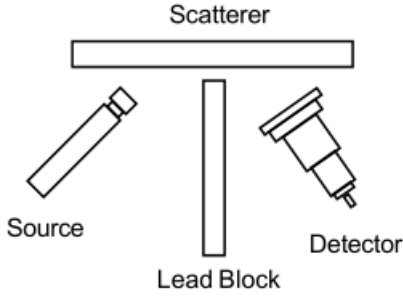


FIG. 18: Schematic diagram for Backscattering experiment



FIG. 19: Experimental set-up for Backscattering experiment

scattering by collisions of Beta particles with electrons in the material. Such a collision changes the speed and direction of the Beta particles. With increasing atomic number Z of the material, the chance that a collision results in a scattering of the Beta particle increases too. Back scattering occurs, when the angle of deflection is greater than 90° . The Back-scattering rate is predominately dependent on the atomic number Z of the back scattering material. With an atom of high atomic number, the scattering occurs at a large angle and with little loss of energy. The back scattering factor is approximately proportional to the square root of atomic number. The mass per unit area (thickness \times density) or the thickness of the irradiated material only influence the back scattering factor up to a saturation value. The maximum back scattering is practically attained at a mass per unit area which is smaller than half the range of the Beta particle in the material, because large layer thicknesses lead to absorption of the scattered electrons. The saturation value is less than 200 mg cm^{-2} for all materials. This corresponds to a saturation larger thickness of $x < 0.74 \text{ mm}$ for Aluminum and $x < 0.17 \text{ mm}$ for Lead.

The equipment required for this experiment are the electronic unit, the wide end window G-M detector, the absorber stand for Back scattering of Beta, absorber set, beta source and Lead block for isolation.

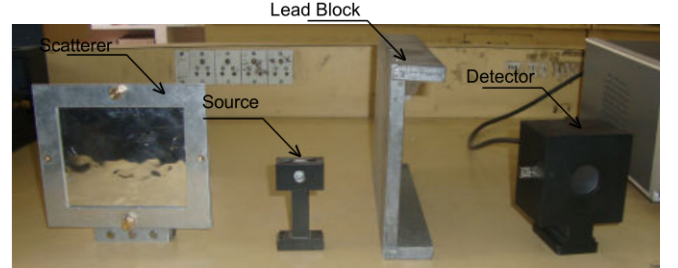


FIG. 20: Individual blocks of experiment setup

TABLE VIII: Reading for Backscattering of Beta particles experiment

Thickness of Al foil (mm)	Counts (200 s)	Net Counts
0	344	0
0.05	587	243
0.1	662	318
0.15	683	339
0.2	767	423
0.25	814	470
0.3	843	499
0.35	878	534
0.4	824	480
0.45	795	451

1. Results

From the obtained results, it can be concluded that the counts due to Back scattering increases up to certain thickness of the scattering material and almost remains constant beyond that thickness. The thickness of the scatterer, where the counts reach their maximum is called the Saturation thickness.

G. Production and Attenuation of Bremsstrahlung

Bremsstrahlung is electromagnetic radiation produced by the deceleration of a charged particle when deflected by another charged particle, typically an electron by an atomic nucleus. The moving particle loses kinetic energy, which is converted into a photon because energy is conserved. The term is also used to refer to the process of producing the radiation. Bremsstrahlung has a continuous spectrum which becomes more intense and whose intensity shifts toward higher frequencies as the change of the energy of the accelerated particles increases.

Beta – particle emitting substances sometimes exhibit a weak radiation with continuous spectrum that is due to Bremsstrahlung. In this context, Bremsstrahlung is a type of *secondary radiation*, in that it is produced as a result of stopping (or slowing) the primary radiation (Beta particles). It is very similar to x-rays produced by

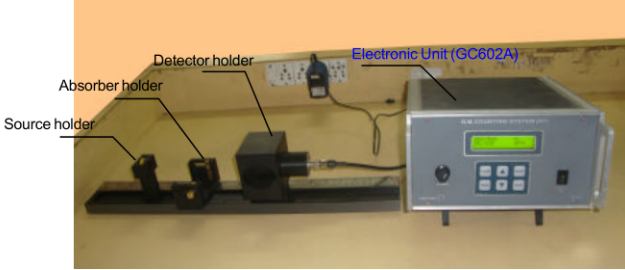


FIG. 21: Experimental set-up for the Bremsstrahlung experiment

TABLE IX: Readings for Bremsstrahlung experiment

(a) For Al (0.7mm) and Perspex (1.8mm) combination:

#	Position	Counts (300 s)	Net Counts
1	Aluminium facing source	798	546
2	Perspex facing source	792	540
3	No Absorber	8342	8090

(b) For Perspex (1.8mm) and Cu (0.3mm) combination:

#	Position	Counts (300 s)	Net Counts
1	Perspex facing source	498	246
2	Copper facing source	535	283
3	No Absorber	8556	8304

(c) For Al (1.8mm) and Cu (0.3mm) combination:

#	Position	Counts (300 s)	Net Counts
1	Aluminium facing source	523	271
2	Copper facing source	542	290
3	No Absorber	8259	8007

bombarding metal targets with electrons in X-ray machines.

The amount of Bremsstrahlung increases as the atomic number/density of the absorbing material goes up. If the mass per unit area (thickness \times density) of the plates used as absorbers is such that the beta particles are completely absorbed, then for materials of higher atomic number/density, correspondingly higher Bremsstrahlung count rates are obtained.

The equipment required for this experiment are the electronic unit, the G-M detector, detector holder, sliding bench, source holder, absorber Holder, beta source and Al (0.7 mm), Cu (0.3 mm) and Perspex (1.8 mm).

1. Discussions

1. The count rate for the Bremsstrahlung produced depends on the order in which the absorbent materials are arranged. If, firstly, the sheet of metal

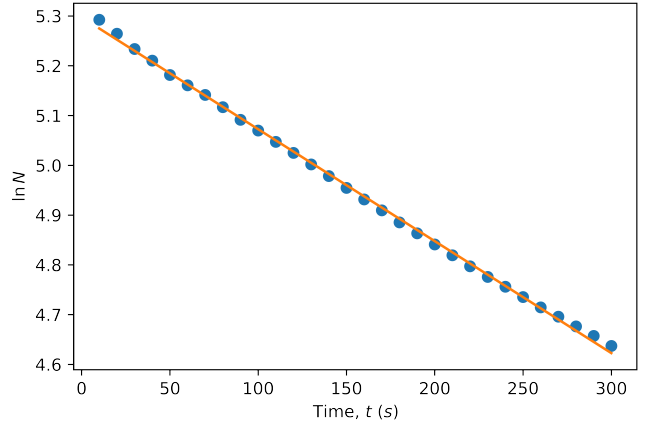


FIG. 22: Plot between $\log S$ and time, t for half-life experiment

faces towards the source, then a higher count rate is measured since Bremsstrahlung is generated in the aluminium but is absorbed to a very small extent in the sheet of Perspex which follows.

2. If, however, the beta rays first strike the sheet of plastic, then the Bremsstrahlung generated is of low energy and a large proportion of it is absorbed in the sheet of metal which follows. These conclusions can be extended to other combinations of materials also.

2. Results

H. Measurement of Short Half-life

The purpose of this experiment is to determine short half-life of a given source, which can be obtained from a mini generator or produced with a neutron source by activation. The equipment required for this experiment are the G-M counting system, the end window detector stand, the G-M detector itself and a short half-life source.

1. Calculations

Intensity of radioactive source changes with time in accordance with relation

$$I = I_0 e^{-\lambda t} \quad (17)$$

where λ is the decay constant, I is the intensity at any time t and I_0 is the initial intensity. The $T_{1/2}$ by definition is the time required for the intensity to fall to one

TABLE X: Readings for short half-life experiment

Elapsed Time (s)	Counts	Corrected counts	Corrected counts, $N (s^{-1})$	$\ln N$
10	2001	1988	199	5.292
20	3892	3866	193	5.264
30	5663	5624	187	5.234
40	7377	7325	183	5.21
50	8961	8896	178	5.181
60	10535	10457	174	5.161
70	12057	11966	171	5.141
80	13447	13343	167	5.117
90	14751	14634	163	5.091
100	16045	15915	159	5.07
110	17256	17113	156	5.047
120	18416	18260	152	5.025
130	19498	19329	149	5.002
140	20514	20332	145	4.978
150	21470	21275	142	4.955
160	22380	22172	139	4.931
170	23268	23047	136	4.909
180	24051	23817	132	4.885
190	24841	24594	129	4.863
200	25577	25317	127	4.841
210	26286	26013	124	4.819
220	26942	26656	121	4.797
230	27578	27279	119	4.776
240	28221	27909	116	4.756
250	28796	28471	114	4.735
260	29345	29007	112	4.715
270	29911	29560	109	4.696
280	30428	30064	107	4.676
290	30925	30548	105	4.657
300	31365	30975	103	4.637

half of its initial value. Hence, we have

$$\begin{aligned} \ln(I/I_0) &= -\lambda T_{1/2} \\ \ln(0.5) &= -\lambda T_{1/2} \\ \frac{0.693}{\lambda} &= T_{1/2} \\ \implies \lambda &= \frac{0.693}{T_{1/2}} \end{aligned} \quad (18)$$

Using the data from table (X), we plot the figure (22). From here we calculate the slope using least square fit as

$$m = \frac{SS_{xy} - S_x S_y}{SS_{xx} - S_x^2} \quad (19)$$

where S is the number of observations, x is the time interval and y is $\ln S$. Putting in the values, we get slope, $m = -224.88 \times 10^{-5} \text{ s}^{-1}$. This slope should be equal to the negative of the decay constant λ as is evident from our formula. Therefore $\lambda = 224.88 \times 10^{-5} \text{ s}^{-1}$. And thus, $T|/2 = 0.693/(224.88 \times 10^{-5}) = 308.2 \text{ s}$ is the short half-life.

2. Error Analysis

We know that error in slope is given by

$$\sigma_m = \sigma_y \sqrt{\frac{S}{\Delta}} \quad (20)$$

Here σ_y is the error in error in $\ln N$ and is equal to 0.01. And $\Delta = SS_{xx} - S_x^2$. Putting in the values we get, $\sigma_m = 2.1 \times 10^{-5} \text{ s}^{-1}$. From here, we can say that, error in $T_{1/2}$ is $dT_{1/2} = 2.87 \text{ s}$.

3. Results

- The decay constant was obtained as $\lambda = (224 \pm 2) \times 10^{-5} \text{ s}^{-1}$ after taking consideration of significant figures.
- The short half-life was obtained as $T_{1/2} = (308 \pm 3) \text{ s}$ after taking consideration of significant figures.

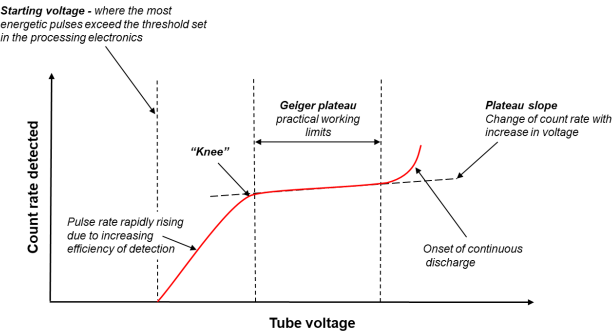


FIG. 23: The characteristic curve of Geiger Muller tube response with constant radiation against varying tube voltage.

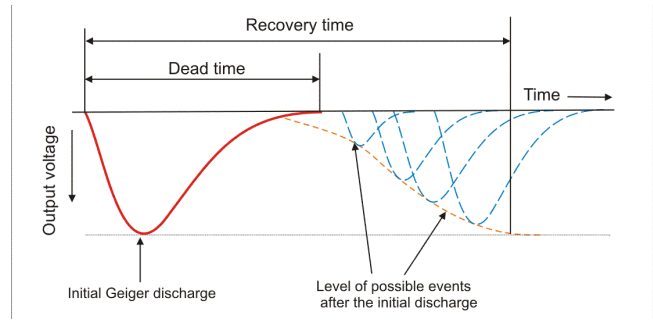


FIG. 24: Dead time and recovery time in a Geiger Muller tube. The tube can produce no further pulses during the dead time, and only produces pulses of lesser height until the recovery time has elapsed.

IV. CONCLUSIONS

1. Almost all of the experiments done were successful and the results obtained were in harmony with the expected/theoretical data and literature.
2. All experiments are conducted on the operating voltage determined through the first experiment where we investigate the G.M. tube characteristic curve.
3. The background counts correspond to the counting rate measured in the absence of the radiation source. It is due to cosmic rays and any active sources in the experimental room.
4. Dead time is the time interval, after the initiation of a discharge resulting in a normal pulse, during which the G.M. Tube is insensitive to further ionizing events.
5. Resolution time is the minimum time interval between two distinct ionizing events which enables both to be counted independently or separately.
6. Recovery time is the minimum time interval between the initiation of a normal size pulse and the

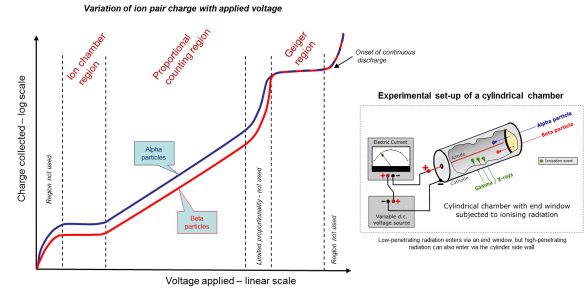


FIG. 25: Practical Gaseous Ionisation detection regions

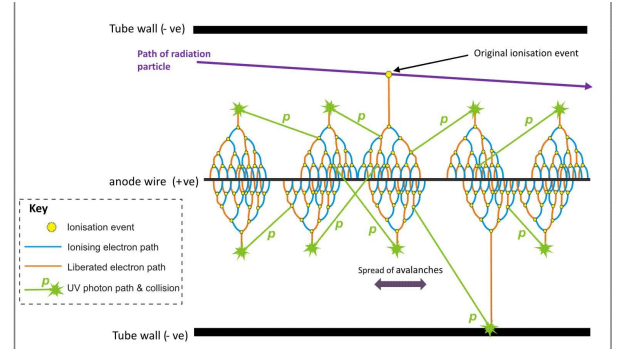


FIG. 26: Visualization of the spread of Townsend avalanches by means of UV photons. This mechanism allows a single ionizing event to ionize all the gas surrounding the anode by triggering multiple avalanches.

initiation of the next pulse of normal size.

7. The figure (25) shows the relationship of the gaseous detection regions, using an experimental concept of applying a varying voltage to a cylindrical chamber which is subjected to ionising radiation. Alpha and beta particles are plotted to demonstrate the effect of different ionising energies, but the same principle extends to all forms of ionising radiation.
8. Normally the tube should be operated with an anode resistor of the value indicated in the measuring circuit, or higher. Decreasing the value of the anode resistor not only decreases the dead time but also the plateau length. A decrease in resistance below the limiting value may affect tube life and lead to its early destruction.
9. Avalanche effect in gas subject to ionising radiation between two plate electrodes. The original ionisation event liberates one electron, and each subsequent collision liberates a further electron, so two electrons emerge from each collision to sustain the avalanche.
10. The anode resistor should be connected directly to the anode connector of the tube to ensure that par-

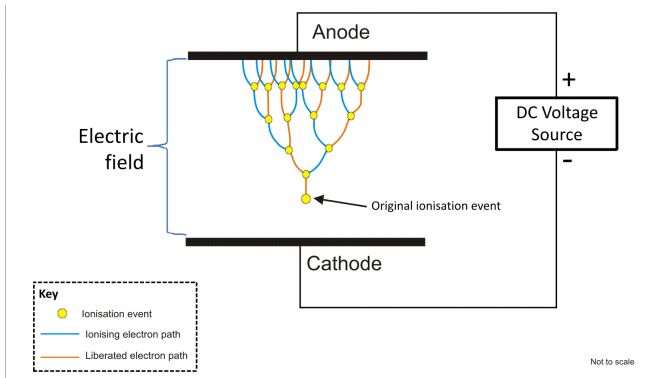


FIG. 27: Visualisation of Townsend avalanche

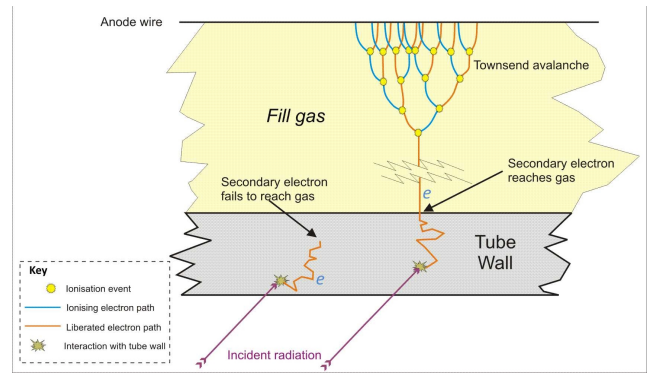


FIG. 28: Detection of gamma in a G-M tube with a thick-walled stainless steel cathode. Secondary electrons generated in the wall can reach the fill gas to produce avalanches.

asitic capacitances of leads will not excessively increase the capacitive load on the tube. An increase in capacitive load may increase the pulse amplitude, the pulse duration, the dead time and plateau slope. In addition the plateau will be shortened ap-

preciably.

11. For continuous stable operation, it is recommended that the counting rate is adjusted to a value in the linear part of the counting rate/dose rate curve.
12. At dose rates exceeding the recommended maximum, a G.M. Tube will produce the maximum number of counting pulses per second, limited by its dead time and the circuit in which it is incorporated. However, due to the characteristics of a specific circuit, the indicated counting rate may fall appreciably, even to zero. If dose rates exceeding 10 times the recommended maximum for window tubes, or 100 times for cylinder tubes, are likely to be encountered, it is advisable to use a circuit that continuously indicates saturation.
13. The most important sources of background count are: Gamma radiation from the environment and from cosmic radiation, mesons from cosmic radiation, beta particles from contamination and impurities of the materials from which the detector itself is made, spontaneous discharge or pulses in the detector and the counting circuit that do not originate from radiation (Electronic noise).
14. The operational life of a G.M. Tube is expressed in counts (discharge). Theoretically the quenching gas, ionized during a discharge, should be recombined between discharges. However, minute quantities will be chemically bound, no longer taking part in the quenching process. This will lead to a gradual reduction of the plateau length and for a given working voltage to an increased counting rate. This will culminate in a continuous state of discharge of the tube rendering it useless.
15. While handling the radioactive sources, utmost precautions should be taken.